10-19-2017

JLab Measurements of the He-3 Form Factors at Large Momentum Transfers

A. Camsonne

A. T. Katramatou

M. Olson

A. Acha

K. Allada

See next page for additional authors

Recommended Citation

Camsonne, A.; Katramatou, A. T.; Olson, M.; Acha, A.; Allada, K.; Anderson, B. D.; Arrington, J.; Baldwin, A.; Chen, J. -P.; Choi, S.; Chudakov, E.; Cisbani, E.; Craver, B.; Decowski, P.; Dutta, C.; Folts, E.; Frullani, S.; Garibaldi, F.; Gilman, R.; Gomez, J.; Hahn, B.; Hansen, J. -O.; Higinbotham, D. W.; Holmstrom, T.; and Kelleher, A., JLab Measurements of the He-3 Form Factors at Large Momentum Transfers (2017). *PHYSICAL REVIEW LETTERS*, 119(16).
10.1103/PhysRevLett.119.162501

Authors
A. Camsonne, A. T. Katramatou, M. Olson, A. Acha, K. Allada, B. D. Anderson, J. Arrington, A. Baldwin, J. -P. Chen, S. Choi, E. Chudakov, E. Cisbani, B. Craver, P. Decowski, C. Dutta, E. Folts, S. Frullani, F. Garibaldi, R. Gilman, J. Gomez, B. Hahn, J. -O. Hansen, D. W. Higinbotham, T. Holmstrom, and A. Kelleher

JLab Measurements of the ^{3}He Form Factors at Large Momentum Transfers

A. Camsonne,[22] A. T. Katramatou,[11] M. Olson,[20] A. Acha,[4] K. Allada,[12] B. D. Anderson,[11] J. Arrington,[1] A. Baldwin,[11] J.-P. Chen,[22] S. Choi,[18] E. Chudakov,[22] E. Cisbani,[8,10] B. Craver,[23] P. Decowski,[19] C. Dutta,[12] E. Folts,[22] S. Frullani,[8,10] F. Garibaldi,[8,10] R. Gilman,[16,22] J. Gomez,[22] B. Hahn,[24] J.-O. Hansen,[22] D. W. Higinbotham,[22] T. Holmstrom,[13] J. Huang,[14] M. Iodice,[9] X. Jiang,[16] A. Kelleher,[24] E. Khrosinkova,[11] A. Kievsky,[7] E. Kuchina,[16] G. Kumbartzki,[16] B. Lee,[18] J. J. LeRose,[22] R. A. Lindgren,[23] G. Lott,[22] H. Lu,[17] L. E. Marcucci,[7,15] D. J. Margaziotis,[2] P. Markowitz,[4] S. Marrone,[6] D. Meekins,[22] Z.-E. Meziani,[21] R. Michaels,[22] B. Moffit,[14] B. Norum,[23] G. G. Petratos,[11] A. Puckett,[14] X. Qian,[3] O. Rondon,[23] A. Saha,[22] B. Sawatzky,[21] J. Segal,[22] M. Shabestari,[23] A. Shahinyan,[25] P. Solvignon,[1] N. Sparveris,[11,21] R. R. Subedi,[23] R. Suleiman,[22] V. Sulkosky,[22] G. M. Urciuoli,[8] M. Viviani,[7] Y. Wang,[5] B. B. Wojtsekhowski,[22] X. Yan,[18] H. Yao,[21] W.-M. Zhang,[11] X. Zheng,[23] and L. Zhu[5]

(The Jefferson Lab Hall A Collaboration)

[1]*Argonne National Laboratory, Argonne, Illinois 60439, USA*
[2]*California State University, Los Angeles, California 90032, USA*
[3]*Duke University (TUNL), Durham, North Carolina 27708, USA*
[4]*Florida International University, Miami, Florida 33199, USA*
[5]*University of Illinois at Urbana Champagne, Urbana, Illinois 61801, USA*
[6]*Istituto Nazionale di Fisica Nucleare, Sezione di Bari and University of Bari, 70126 Bari, Italy*
[7]*Istituto Nazionale di Fisica Nucleare, Sezione di Pisa, 56127 Pisa, Italy*
[8]*Istituto Nazionale di Fisica Nucleare, Sezione di Roma, 00185 Rome, Italy*
[9]*Istituto Nazionale di Fisica Nucleare, Sezione di Roma Tre, 00146 Rome, Italy*
[10]*Istituto Superiore di Sanità, 00161 Rome, Italy*
[11]*Kent State University, Kent, Ohio 44242, USA*
[12]*University of Kentucky, Lexington, Kentucky 40506, USA*
[13]*Longwood University, Farmville, Virginia 23909, USA*
[14]*Massachusetts Institute of Technology, Cambridge, Massachusetts 02139, USA*
[15]*University of Pisa, 56127 Pisa, Italy*
[16]*Rutgers, The State University of New Jersey, Piscataway, New Jersey 08855, USA*
[17]*University of Science and Technology of China, Hefei, Anhui 230026, People's Republic of China*
[18]*Seoul National University, Seoul 151-747, Korea*
[19]*Smith College, Northampton, Massachusetts 01063, USA*
[20]*St. Norbert College, De Pere, Wisconsin 54115, USA*
[21]*Temple University, Philadelphia, Pennsylvania 19122, USA*
[22]*Thomas Jefferson National Accelerator Facility, Newport News, Virginia 23606, USA*
[23]*University of Virginia, Charlottesville, Virginia 22904, USA*
[24]*College of William and Mary, Williamsburg, Virginia 23185, USA*
[25]*Yerevan Physics Institute, Yerevan 375036, Armenia*

(Received 31 October 2016; published 19 October 2017; publisher error corrected 3 November 2017)

The charge and magnetic form factors, F_C and F_M, respectively, of ^{3}He are extracted in the kinematic range 25 fm$^{-2} \leq Q^2 \leq 61$ fm^{-2} from elastic electron scattering by detecting ^{3}He recoil nuclei and scattered electrons in coincidence with the two High Resolution Spectrometers of the Hall A Facility at Jefferson Lab. The measurements find evidence for the existence of a second diffraction minimum for the magnetic form factor at $Q^2 = 49.3$ fm^{-2} and for the charge form factor at $Q^2 = 62.0$ fm^{-2}. Both minima are predicted to exist in the Q^2 range accessible by this Jefferson Lab experiment. The data are in qualitative agreement with theoretical calculations based on realistic interactions and accurate methods to solve the three-body nuclear problem.

DOI: 10.1103/PhysRevLett.119.162501

Elastic electron scattering from nuclei has been a basic tool in the study of their size and associated charge and magnetization distributions [1]. It has provided precise measurements of the charge and magnetic radius of nuclei, starting with the seminal experiments of Hofstadter and collaborators at Stanford in the 1950s [2]. Elastic scattering

measurements determine the nuclear electromagnetic (EM) form factors, which in the case of few-body nuclei can be compared with state-of-the-art theoretical calculations. The latter are based on sophisticated models that solve for the few-body nuclear wave functions using modern nucleon-nucleon potentials. The framework used is that of the impulse approximation (IA), where the electron interacts through virtual photon exchange with just one of the nucleons in the target nucleus, complemented by the inclusion of meson exchange among the nucleons.

The few-body EM form factors are considered the "observables of choice" [3] for testing the nucleon-meson standard model of the nuclear interaction and the associated EM current operator [4]. In general, they provide fundamental information on the internal structure and dynamics of light nuclei, as they are, at the simplest level, convolutions of the nuclear ground state wave function with the EM form factors of the constituent nucleons.

The theoretical calculations for these few-body observables are very sensitive to the model used for the nuclear EM current operator, especially its meson-exchange-current (MEC) contributions. Relativistic corrections and possible admixtures of multiquark states in the nuclear wave function might also be relevant [4,5]. Additionally, at large momentum transfers, these EM form factors may offer a unique opportunity to uncover a possible transition in the description of elastic electron scattering by few-body nuclear systems, from meson-nucleon to quark-gluon degrees of freedom, as predicted originally by the dimensional-scaling quark model (DSQM) [6]. The field theory approach of the DSQM, later substantiated within the perturbative QCD framework [7], is based on dimensional scaling of high-energy amplitudes using quark counting. This leads to a prediction for an asymptotic form factor falloff at large Q^2. For example, in the ^{3}He case, the $A(Q^2)$ elastic structure function (see below) is predicted to fall as $\sqrt{A(Q^2)} \sim (Q^2)^{-8}$ [6]. The conclusions of this work offer valuable input on the applicability of the above theoretical frameworks.

Experimentally, the few-body form factors are determined from elastic electron-nucleus scattering using high-intensity beams, high-density targets, and large solid angle magnetic spectrometers. There have been extensive experimental investigations of the few-body form factors over the past 50 years at almost every electron accelerator laboratory [8,9], complemented by equally extensive theoretical calculations and predictions [4,9–11]. The investigation of their behavior at large momentum transfers has been an integral part of the nuclear structure program of Jefferson Lab (JLab) since its inception [12].

This work focuses on a measurement of the ^{3}He EM form factors at JLab. The cross section for elastic scattering of a relativistic electron from the spin-1/2 ^{3}He nucleus is given, in the one-photon exchange approximation and in natural units, by the formula [13]

$$\frac{d\sigma}{d\Omega} = \left(\frac{d\sigma}{d\Omega}\right)_{NS} \left[A(Q^2) + B(Q^2)\tan^2\left(\frac{\theta}{2}\right)\right], \quad (1)$$

where

$$\left(\frac{d\sigma}{d\Omega}\right)_{NS} = \frac{(Z\alpha)^2 E' \cos^2(\frac{\theta}{2})}{4E^3 \sin^4(\frac{\theta}{2})} \quad (2)$$

is the cross section for the scattering of a relativistic electron by a structureless nucleus and A and B are the elastic structure functions of ^{3}He:

$$A(Q^2) = \frac{F_C^2(Q^2) + \mu^2 \tau F_M^2(Q^2)}{1+\tau}, \quad (3)$$

$$B(Q^2) = 2\tau\mu^2 F_M^2(Q^2), \quad (4)$$

with F_C and F_M being the charge and magnetic form factors, respectively, of the nucleus. Here, α is the fine-structure constant, Z and μ are the nuclear charge and magnetic moment, respectively, E and E' are the incident and scattered electron energies, respectively, θ is the electron scattering angle, $Q^2 = 4EE'\sin^2(\theta/2)$ is minus the four-momentum transfer squared, and $\tau = Q^2/4M^2$ with M being the nuclear mass.

The three-body form factors have been theoretically investigated by several groups, using different techniques to solve for the nuclear ground states and a variety of models for the nuclear EM current [14–17]. The most recent calculation of the ^{3}H and ^{3}He form factors in the Q^2 range of the experiment is that of Refs. [3,18]. It uses the pair-correlated hyperspherical harmonics (HH) method [19] to construct high-precision nuclear wave functions and goes beyond the IA by including MEC, whose main contributions are constructed to satisfy the current conservation relation with the given Hamiltonian [18]. Part of the present work is the extension of the above method to evolve the ^{3}He F_C and F_M form factors (see Figs. 1–3) to large momentum transfers, using ^{3}He wave functions obtained from the Argonne AV18 nucleon-nucleon and Urbana UIX three-nucleon interactions [20]. The calculations include MEC contributions arising from π-, ρ-, and ω-meson exchanges, as well as the $\rho\pi\gamma$ and $\omega\pi\gamma$ charge transition couplings. A recent review is given in Ref. [11].

The experiment (E04-018, which also measured the ^{4}He charge form factor [21]) used the Continuous Electron Beam Accelerator and Hall A Facilities of JLab. Electrons scattered from a high-density cryogenic ^{3}He target were detected in the Left High Resolution Spectrometer (e-HRS). To suppress backgrounds and unambiguously separate elastic from inelastic processes, recoil helium nuclei were detected in the Right HRS (h-HRS) in coincidence with the scattered electrons. The incident-beam energy ranged between 0.688 and 3.304 GeV. The beam current ranged between 19.0 and

99.3 μA. The cryogenic target system contained gaseous ^{3}He and liquid hydrogen cells of length $T = 20.0$ cm. The ^{3}He gas was pressurized to 13.7–14.2 atm at a temperature of 7.1–8.7 K, resulting in a density of 0.057–0.070 g/cm^3. Two Al foils separated by 20.0 cm were used to measure any possible contribution to the cross section from the Al end caps of the target cells.

Scattered electrons were detected in the e-HRS using two planes of scintillators to form an "electron" trigger, a pair of drift chambers for electron track reconstruction, and a gas threshold Čerenkov counter and a lead-glass calorimeter for electron identification. Recoil helium nuclei were detected in the h-HRS using two planes of scintillators to form a "recoil" trigger and a pair of drift chambers for recoil track reconstruction. The event trigger consisted of a coincidence between the two HRS triggers. Details on the Hall A Facility and all associated instrumentation used are given in Ref. [22].

Particles in the e-HRS were identified as electrons on the basis of a minimal pulse height in the Čerenkov counter and the energy deposited in the calorimeter, consistent with the momentum as determined from the drift chamber track using the spectrometer's optical properties. Particles in the h-HRS were identified as ^{3}He nuclei on the basis of their energy deposition in the first scintillator plane. Electron-^{3}He (e-^{3}He) coincidence events, consistent with elastic kinematics, were identified using the relative time-of-flight between the electron and recoil triggers after imposing the above particle identification "cuts." To check the overall normalization, elastic e-proton (e-p) scattering in coincidence was measured at several kinematics. The e-p data are in excellent agreement with the world data, as described in Ref. [21].

The elastic e-^{3}He cross section values were calculated using the formula

$$\left(\frac{d\sigma}{d\Omega}(E,\theta)\right)_{\rm exp} = \frac{N_{\rm er} C_{\rm cor}}{N_b N_t (\Delta\Omega)_{\rm MC} F(Q^2,T)}, \qquad (5)$$

where $N_{\rm er}$ is the number of electron-recoil ^{3}He elastic events, N_b is the number of incident beam electrons, N_t is the number of target nuclei/cm^2, $(\Delta\Omega)_{\rm MC}$ is the effective coincidence solid angle (which includes most radiative effects) from a Monte Carlo simulation, F is the portion of the radiative corrections that depends only on Q^2 and T (1.07–1.10) [23], and $C_{\rm cor} = C_{\rm det} C_{\rm cdt} C_{\rm rni} C_{\rm den}$. Here, $C_{\rm det}$ is the correction for the inefficiency of the Čerenkov counter and the calorimeter (1.01) (the scintillator counter hodoscopes were found to be essentially 100% efficient), $C_{\rm cdt}$ is the computer dead-time correction (1.04–1.56), $C_{\rm rni}$ is a correction for losses of recoil nuclei due to nuclear interactions in the target cell and vacuum windows (1.02–1.08), and $C_{\rm den}$ is a correction to the target density due to beam heating effects (ranging between 1.01 at 19 μA and 1.07 at 99 μA). There were no contributions to the elastic e-^{3}He cross section from events originating in the target cell end caps, as determined from runs with the empty replica target. The e-p elastic cross section values were determined similarly.

The effective coincidence solid angle was evaluated with a Monte Carlo computer code that simulated elastic electron-nucleus scattering under identical conditions as

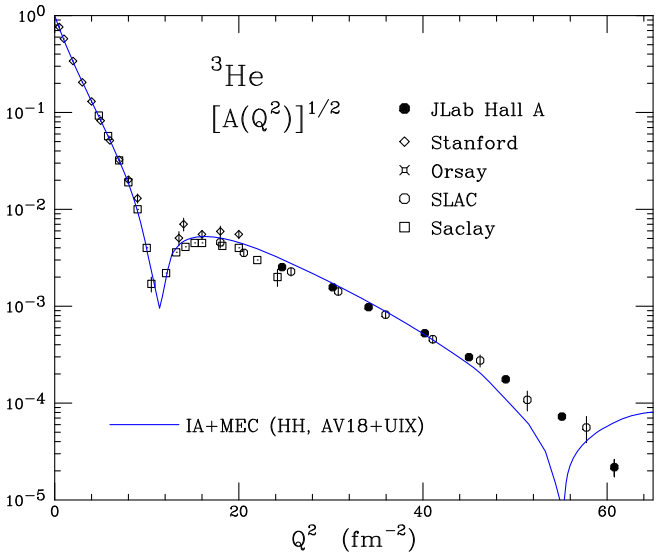

FIG. 1. ^{3}He elastic structure function $A(Q^2)$ data from this experiment, compared to selected previous data and the present theoretical calculation using the hyperspherical harmonics variational method (see the text).

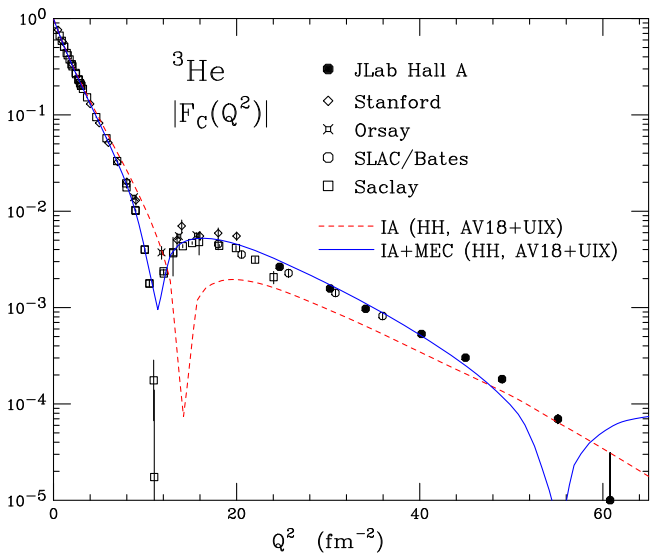

FIG. 2. Absolute values of the ^{3}He charge form factor F_C, as determined from this experiment. Also shown are selected previous data and the present theoretical calculation using the hyperspherical harmonics variational method (see the text).

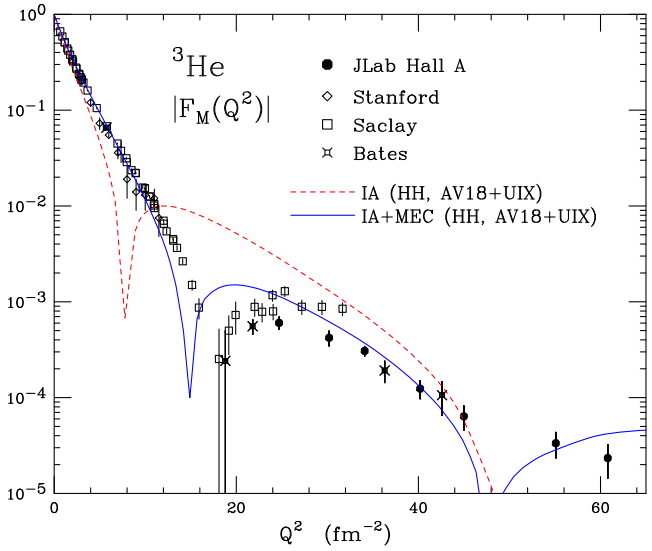

FIG. 3. Absolute values of the ^{3}He magnetic form factor F_M, as determined from this experiment. Also shown are selected previous data and the present theoretical calculation using the hyperspherical harmonics variational method (see the text).

our measurements [23]. The code tracked scattered electrons and recoil nuclei from the target to the detectors through the two HRS systems using optical models based on magnetic field measurements and precision position surveys of their elements. The effects from ionization energy losses and multiple scattering in the target and vacuum windows were taken into account for both incident and scattered electrons, and recoil nuclei. Bremsstrahlung radiation losses for both incident and scattered electrons in the target and vacuum windows, as well as internal radiative effects, were also taken into account. It should be noted that the two-photon exchange effect is not included in the radiative corrections implementation. A credible correction to the data for this effect should be based on established complementary calculations, which are not yet fully available for the entire kinematic range of our measurements. Although a correction will have to wait for the completion and further understanding of ongoing calculations [24], the latter indicate that at least for the charge form factor the effect can be on the order of a few percent.

The Rosenbluth cross section formula (1) is based on the assumption that the wave functions of the incident and scattered electrons are described by plane waves. In reality, the charge of the nucleus distorts these wave functions, necessitating a correction to the formula [1]. This Coulomb effect shifts the Q^2 value of the interaction to an "effective" value, given by $Q^2_{\rm eff} = (1 + 3Z\alpha\hbar c/2R_{\rm eq}E)^2Q^2$, where $R_{\rm eq}$ is the hard sphere equivalent radius of the nucleus, $\hbar$ is the Planck constant, and c is the speed of light. This correction allows for a form factor extraction using a Rosenbluth separation of cross section values determined at the same $Q^2_{\rm eff}$ [25]. This approach was followed in this experiment, and the results are given in terms of the effective Q^2 in Tables I and II and are plotted in Figs. 1–3.

At each kinematic point, the "reduced" cross section $(d\sigma/d\Omega)_r$, defined using Eqs. (1)–(4) and the experimentally determined cross section $(d\sigma/d\Omega)_{\rm exp}$

$$\left(\frac{d\sigma}{d\Omega}\right)_r = \left(\frac{d\sigma}{d\Omega}\right)_{\rm exp}\left(\frac{d\sigma}{d\Omega}\right)^{-1}_{NS}(1+\tau) = \left(F_C^2 + \mu^2\frac{\tau}{\epsilon}F_M^2\right), \tag{6}$$

was plotted, at the same values of $Q^2_{\rm eff}$, versus $\mu^2\tau/\epsilon$ (Rosenbluth plot), and the ^{3}He F_C^2 and F_M^2 values were extracted by a linear fit. Here, $\epsilon = [1 + 2(1+\tau)\tan^2(\theta/2)]^{-1}$ is the degree of the longitudinal polarization of the exchanged virtual photon. It should be noted that, at $Q^2 = 49.0$ fm^{-2}, data were taken only at a forward angle (25.47°). In this case, the F_C value was extracted under the safe assumption that the F_M does not contribute to the cross section, as it is essentially zero (see Fig. 4).

The $A(Q^2)$ values from this experiment are shown in Fig. 1 along with previous data from a SLAC experiment [26], which performed elastic scattering at a fixed angle $\theta = 8°$, and selected data from other laboratories [25,27,28]. It is evident that the JLab and SLAC data sets are in excellent agreement. Also shown is the present IA + MEC theoretical calculation (see below). The absolute values of the ^{3}He F_C and F_M from this work are shown in Figs. 2 and 3, along with previous Stanford [25], Orsay

TABLE I. Values of the beam energy, scattering angle, effective Q^2, and elastic e-^{3}He cross section with the total error (statistical and systematic added in quadrature).

E (GeV)	θ (deg.)	Q^2 (fm^{-2})	$d\sigma/d\Omega$ (cm^2/sr)
3.304	17.52	24.7	$(2.29 \pm 0.12) \times 10^{-35}$
0.7391	97.78	24.7	$(2.80 \pm 0.20) \times 10^{-37}$
3.304	19.50	30.2	$(5.16 \pm 0.29) \times 10^{-36}$
0.7391	118.99	30.2	$(3.95 \pm 0.38) \times 10^{-38}$
0.6876	139.99	30.2	$(1.51 \pm 0.19) \times 10^{-38}$
3.304	20.83	34.1	$(1.57 \pm 0.10) \times 10^{-36}$
0.8157	113.01	34.1	$(1.43 \pm 0.13) \times 10^{-38}$
0.7394	139.91	34.1	$(6.41 \pm 0.59) \times 10^{-39}$
3.304	22.82	40.2	$(3.03 \pm 0.21) \times 10^{-37}$
0.8177	139.53	40.2	$(1.24 \pm 0.16) \times 10^{-39}$
3.304	24.28	45.0	$(7.56 \pm 0.75) \times 10^{-38}$
0.9330	119.94	45.0	$(6.84 \pm 1.10) \times 10^{-40}$
0.8726	140.66	45.0	$(3.24 \pm 0.51) \times 10^{-40}$
3.304	25.47	49.0	$(2.13 \pm 0.35) \times 10^{-38}$
3.304	27.24	55.1	$(2.77 \pm 0.39) \times 10^{-39}$
0.9893	140.31	55.1	$(3.27 \pm 0.13) \times 10^{-41}$
3.304	28.86	60.8	$(2.14 \pm 0.72) \times 10^{-40}$
1.052	140.51	60.8	$(1.13 \pm 0.80) \times 10^{-41}$

TABLE II. Effective Q^2 and ^{3}He charge and magnetic form factors (absolute values) with total errors (statistical and systematic added in quadrature).

Q^2 (fm^{-2})	$\lvert F_C\rvert$	$\lvert F_M\rvert$
24.7	$(2.65 \pm 0.06) \times 10^{-3}$	$(6.03 \pm 0.91) \times 10^{-4}$
30.2	$(1.58 \pm 0.05) \times 10^{-3}$	$(4.21 \pm 0.75) \times 10^{-4}$
34.1	$(9.73 \pm 0.34) \times 10^{-4}$	$(3.07 \pm 0.35) \times 10^{-4}$
40.2	$(5.32 \pm 0.21) \times 10^{-4}$	$(1.24 \pm 0.27) \times 10^{-4}$
45.0	$(3.02 \pm 0.16) \times 10^{-4}$	$(6.37 \pm 1.83) \times 10^{-5}$
49.0	$(1.81 \pm 0.15) \times 10^{-4}$	–
55.1	$(6.97 \pm 0.72) \times 10^{-5}$	$(3.34 \pm 1.00) \times 10^{-5}$
60.8	$(1.00 \pm 2.10) \times 10^{-5}$	$(2.34 \pm 0.90) \times 10^{-5}$

[27], SLAC [26], Saclay [28], and MIT/Bates [29] data. Not shown, for clarity, are the low Q^2 MIT/Bates data [30]. In all three figures, the error bars represent statistical and systematic uncertainties added in quadrature. The new F_C data are in excellent agreement with data extracted from a Rosenbluth separation between SLAC forward angle ($\theta = 8°$) cross sections and interpolations of backward angle (160°) MIT/Bates cross sections [29], labeled as "SLAC/Bates" data in Fig. 2. The new F_M data are in excellent agreement with the MIT/Bates data taken at $\theta = 160°$ but in very strong disagreement with the Saclay data taken at $\theta = 155°$. The F_M datum at $Q^2 = 24.7$ fm^{-2} has been extracted from a Rosenbluth separation of a forward- and a medium-θ JLab-measured cross section and an interpolated cross section from the high-quality $\theta = 160°$ MIT/Bates data set [29,31].

The new JLab data of Figs. 2 and 3 indicate the presence of an apparent second diffraction minimum for the F_M in the vicinity of $Q^2 = 50$ fm^{-2} and the onset of a second diffraction minimum for the F_C located at a Q^2 value just beyond 60 fm^{-2}. To further substantiate the existence of the two minima, the algebraic values of the ^{3}He F_C and F_M form factors have been plotted on a linear scale and over a selected Q^2 range, as shown in Fig. 4. Here it is implicitly assumed that the ^{3}He F_C and F_M become negative after crossing their first diffraction minimum at $Q^2 = 11$ and 17 fm^{-2}, respectively. For comparison, also shown in Fig. 4 are the algebraic values of the charge form factor of ^{4}He [21]. An interpolation of the new JLab data in Fig. 4 shows that the ^{3}He F_M crosses zero for a second time at $Q^2 = 49.3$ fm^{-2} and then becomes positive. An extrapolation of the new JLab data in Fig. 4 shows that the ^{3}He F_C crosses zero for a second time at a Q^2 value of 62.0 fm^{-2} and then presumably becomes positive.

An updated extension of the latest theoretical calculation based on the IA with the inclusion of MEC, which used the HH variational method to calculate the ^{3}He wave function, as described above and outlined in Ref. [18], was performed for this work and is shown in Figs. 2 and 3. The calculation is, in general, in qualitative agreement with the

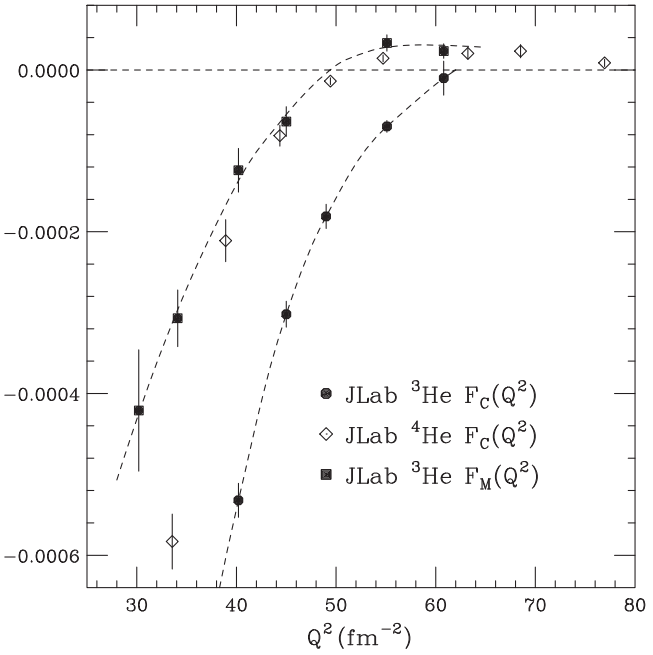

FIG. 4. Algebraic values of the ^{3}He charge and magnetic form factors over a selected Q^2 range. Also shown are algebraic values of the ^{4}He charge form factor over the same Q^2 range [21]. The dashed lines have been drawn to just guide the eye through the data.

data even at large momentum transfers, where theoretical uncertainties may become sizable (estimated to be, for example, at $Q^2 = 60$ fm^{-2}, on the order of $\pm 30\%$ for both form factors). Of note is the long-standing disagreement between the calculation and the data in the Q^2 range around the first diffraction minimum of the ^{3}He F_M. It is not presently clear if this is due to a missing piece of important physics in the nonrelativistic theory or to the need for a fully relativistic calculation. The presently available relativistic calculation based on the Gross equation [32] will be able to be compared to the new data when the not-yet-calculated $\rho\pi\gamma$ interaction current is included in this so-called "relativistic impulse approximation" approach [11].

It should be noted that all seminal, older calculations of the ^{3}He form factors (not shown in Figs. 2 and 3) based on the Faddeev formalism [14,15] or the Monte Carlo variational method [16,17] are in qualitative agreement with the data in predicting a diffractive structure for both form factors and also indicative, in general, of large MEC contributions. Also, it is evident that the diffractive pattern of the JLab data is incompatible with the asymptotic-falloff DSQM prediction [6] and that it supports the conclusion of Ref. [33] that the onset of asymptotic scaling must be at a Q^2 value much greater than 100 fm^{-2}, not presently accessible at JLab for ^{3}He.

In summary, we have measured the ^{3}He charge and magnetic form factors in the range 25 fm$^{-2} \leq Q^2 \leq 61$ fm^{-2}. The results are in qualitative agreement with theoretical

calculations based on the IA with inclusion of MEC. These new data support the existence of a second diffraction minimum for both form factors, located at $Q^2 = 62.0$ fm^{-2} for the F_C case and at $Q^2 = 49.3$ fm^{-2} for the F_M case. The new large Q^2 ^{3}He form factor results will constrain inherent uncertainties in the theoretical calculations and lead, together with previous large Q^2 data on the deuteron [34,35], tritium [28], and ^{4}He [21] EM form factors, to the development of a consistent hadronic model describing the internal EM structure and dynamics of few-body nuclear systems.

We acknowledge the outstanding support of the staff of the Accelerator and Physics Divisions of JLab that made this experiment possible. We are grateful to Dr. D. Riska, Dr. R. Schiavilla, and Dr. R. Wiringa for kindly providing their theoretically motivating calculations for the proposal of this experiment and to Dr. F. Gross, Dr. R. Schiavilla, and Dr. W. Melnitchouk for valuable discussions and support. This material is based upon work supported by the U.S. Department of Energy (DOE), Office of Science, Office of Nuclear Physics under Contract No. DE-AC05-060R23177. This work was also supported by DOE Awards No. DE-AC02-06CH11357 and No. DE-FG02-96ER40950, National Science Foundation Grants No. NSF-PHY-0701679, No. NSF-PHY-1405814, No. NSF-PHY-1714809, and No. NSF-PHY-0652713, the Kent State University Research Council, and the INFN.

[1] Herbert Uberall, *Electron Scattering from Complex Nuclei* (Academic Press, New York, 1971).
[2] R. Hofstadter, Annu. Rev. Nucl. Part. Sci. **7**, 231 (1957).
[3] L. E. Marcucci, D. O. Riska, and R. Schiavilla, Phys. Rev. C **58**, 3069 (1998).
[4] J. Carlson and R. Schiavilla, Rev. Mod. Phys. **70**, 743 (1998), and references therein.
[5] H. Dijk and B. L. G. Bakker, Nucl. Phys. **A531**, 555 (1991), and references therein.
[6] S. J. Brodsky and B. T. Chertok, Phys. Rev. D **14**, 3003 (1976); B. T. Chertok, Phys. Rev. Lett. **41**, 1155 (1978).
[7] S. J. Brodsky and C.-R. Ji, Prog. Part. Nucl. Phys. **13**, 299 (1985), and references therein.
[8] I. Sick, Prog. Part. Nucl. Phys. **47**, 245 (2001).
[9] R. Gilman and F. Gross, J. Phys. G **28**, R37 (2002).
[10] R. J. Holt and R. Gilman, Rep. Prog. Phys. **75**, 086301 (2012).
[11] L. E. Marcucci, F. Gross, M. T. Peña, M. Piarulli, R. Sciavilla, I. Sick, A. Stadler, J. W. Van Orden, and M. Viviani, J. Phys. G **43**, 023002 (2016).
[12] P. D. Barnes *et al.*, report of the DOE/NSF Nuclear Science Advisory Committee, 1982.
[13] E. Hadjimichael, *International Review of Nuclear Physics*, (World Scientific, Singapore, 1985), Vol. 3.
[14] E. Hadjimichael, B. Goulard, and R. Bornais, Phys. Rev. C **27**, 831 (1983); E. Hadjimichael, Phys. Lett. B **172**, 156 (1986).
[15] W. Strueve, Ch. Hadjuk, P. U. Sauer, and W. Theis, Nucl. Phys. **A465**, 651 (1987).
[16] R. Schiavilla, V. R. Pandharipande, and D. O. Riska, Phys. Rev. C **40**, 2294 (1989); **41**, 309 (1990).
[17] R. B. Wiringa, Phys. Rev. C **43**, 1585 (1991).
[18] L. E. Marcucci, M. Viviani, R. Schiavilla, A. Kievsky, and S. Rosati, Phys. Rev. C **72**, 014001 (2005).
[19] A. Kievsky, S. Rosati, M. Viviami, L. E. Marcucci, and L. Girlanda, J. Phys. G **35**, 063101 (2008), and references therein.
[20] R. B. Wiringa, V. G. J. Stoks, and R. Schiavilla, Phys. Rev. C **51**, 38 (1995); B. S. Pudliner, V. R. Pandharipande, J. Carlson, S. C. Pieper, and R. B. Wiringa, Phys. Rev. C **56**, 1720 (1997).
[21] A. Camsonne *et al.*, Phys. Rev. Lett. **112**, 132503 (2014).
[22] J. Alcorn *et al.*, Nucl. Instrum. Methods Phys. Res., Sect. A **522**, 294 (2004).
[23] A. T. Katramatou, Kent State University preprint Report No. KSU-CNR-14-11, 2011.
[24] P. G. Blunden, W. Melnitchuk, and J. A. Tjon, Phys. Rev. C **81**, 018202 (2010); A. P. Kobushkin and Ju. V. Timoshenko, Phys. Rev. C **88**, 044002 (2013); A. P. Kobushkin and W. Melnitchouk (private communication).
[25] J. S. McCarthy, I. Sick, and R. R. Whitney, Phys. Rev. C **15**, 1396 (1977), and references therein.
[26] R. G. Arnold, B. T. Chertok, S. Rock, W. P. Schütz, Z. M. Szalata, D. Day, J. S. McCarthy, F. Martin, B. A. Mecking, I Sick, and G. Tamas, Phys. Rev. Lett. **40**, 1429 (1978).
[27] M. Bernheim, D. Blum, W. McGill, R. Riskalla, C. Trail, T. Stovall, and D. Vinciguerra, Lett. Nuovo Cimento Soc. Ital. Fis. **5**, 431 (1972).
[28] A. Amroun *et al.*, Nucl. Phys. **A579**, 596 (1994), and references therein.
[29] I. Nakagawa *et al.*, Phys. Rev. Lett. **86**, 5446 (2001).
[30] P. C. Dunn, S. B. Kowalski, F. N. Rad, C. P. Sargent, W. E. Turchinetz, R. Goloskie, and D. P. Saylor, Phys. Rev. C **27**, 71 (1983); D. H. Beck *et al.*, Phys. Rev. C **30**, 1403 (1984).
[31] I. Nakagawa, Ph.D. thesis, Tohoku University, 1999.
[32] S. A. Pinto, A. Stadler, and F. Gross, Phys. Rev. C **79**, 054006 (2009); **81**, 014007 (2010).
[33] R. J. Holt, Phys. Rev. C **41**, 2400 (1990).
[34] L. C. Alexa *et al.*, Phys. Rev. Lett. **82**, 1374 (1999), and references therein.
[35] P. E. Bosted *et al.*, Phys. Rev. C **42**, 38 (1990).